


M. KÖHL   
 A. ÖTTL  
 S. RITTER  
 T. DONNER  
 T. BOURDEL  
 T. ESSLINGER

# Time interval distributions of atoms in atomic beams

Institute for Quantum Electronics, ETH Zürich, 8093 Zürich, Switzerland

**Received: 6 July 2006**

**Published online: 8 December 2006 • © Springer-Verlag 2006**

**ABSTRACT** We report an experimental investigation of two-particle correlations between neutral atoms in a Hanbury Brown and Twiss experiment. Both an atom laser beam and a pseudo-thermal atomic beam are extracted from a Bose–Einstein condensate and the atom flux is measured with a single atom counter. We determine the conditional and the unconditional detection probabilities for the atoms in the beam and find good agreement with the theoretical predictions.

PACS 03.75.Pp; 05.30.Jp; 07.77.Gx; 42.50.Pq

## 1 Introduction

Hanbury Brown and Twiss experiments [1] play a central role in investigating correlations between identical particles. The underlying idea of these experiments is that intensity fluctuations and their correlations are tightly linked to the quantum mechanical state of a system. The statistical properties of a beam of photons or atoms can be accessed in counting experiments. A famous example of how the statistics vary for different quantum states of light is the distinct difference of photon correlations in thermal light beams and laser beams [2, 3].

For ideal bosonic atoms the same quantum statistical properties are expected as for the case of photons. First experiments investigating the second-order correlation function of laser-cooled thermal atoms have already been undertaken several years ago and the bunching behavior could be observed [4]. The availability of quantum degenerate atomic gases [5] has added a new dimension, since now even coherent states of matter can be investigated. Recently, the second-order correlation function  $g^2(\tau)$  of quantum degenerate atoms has been observed [6, 7] and the feasibility of studying Hanbury Brown and Twiss correlations of atoms released from an optical lattice has been demonstrated [8, 9]. Moreover, atom–atom correlations have also been observed in the dissociation process of ultra-cold molecules [10] and density correlations have been investigated in phase-fluctuating Bose–Einstein condensates (BECs) [11, 12].

The second-order temporal correlation function of the stationary field  $\psi$ ,

$$g^2(\tau) = \frac{\langle \psi^\dagger(\tau) \psi^\dagger(0) \psi(0) \psi(\tau) \rangle}{\langle \psi^\dagger(0) \psi(0) \rangle^2}, \quad (1)$$

reveals valuable information about the intensity noise and the two-particle correlations in the sample. In particular, for an atomic beam released from a Bose–Einstein condensate the correlation function was found to be equal to unity, revealing the second-order coherence of the atomic beam [6]. Together with the measurement of the first-order coherence of this beam [13], this showed that atomic beams extracted from a Bose–Einstein condensate indeed are the matter wave analogue of an optical laser.

In this paper we discuss the two-particle correlations of atoms in an atomic beam extracted from a Bose–Einstein condensate. We measure the conditional and the unconditional probabilities for atom detection, which constitutes a complementary view of two-particle correlations as compared to an analysis of the second-order correlation function.

## 2 Experimental setup

Our experimental setup combines the techniques for the production of atomic Bose–Einstein condensates with single atom detection by means of an ultra-high-finesse optical cavity [6, 14]. We collect  $10^9$   $^{87}\text{Rb}$  atoms in a vapor cell magneto-optical trap which is loaded from a pulsed dispenser source. After polarization gradient cooling and optical pumping into the  $|F = 1, m_F = -1\rangle$  hyperfine ground state, we magnetically transfer the atoms over a distance of 8 cm into a magnetic Quadrupole Ioffe Configuration (QUIC) trap [15]. In this magnetic trap we perform radio-frequency-induced evaporative cooling of the atomic cloud and obtain almost pure Bose–Einstein condensates of  $2 \times 10^6$  atoms. After evaporation we relax the confinement of the atoms to the final trapping frequencies  $(\omega_x, \omega_y, \omega_z) = 2\pi \times (39, 7, 29)\text{Hz}$ , where  $z$  denotes the vertical axis.

For output coupling of an atom laser beam, we apply a weak continuous microwave field to locally spin flip atoms inside the Bose–Einstein condensate into the  $|F = 2, m_F = 0\rangle$  state. These atoms do not experience the magnetic trapping potential but are released from the trap and form a well-collimated beam which propagates downwards due to grav-

✉ Fax: +41-44-633 1254, E-mail: koehl@phys.ethz.ch

ity [16]. The output coupling is performed near the center of the Bose condensate for a duration of 500 ms during which we extract about  $3 \times 10^3$  atoms.

Alternatively, we create a beam with pseudo-thermal correlations from a Bose–Einstein condensate. This is in close analogy to changing the coherence properties of a laser beam by means of a rotating ground glass disk [2, 17]. Instead of applying a monochromatic microwave field for output coupling we use a broadband microwave field. We employ a white-noise radio-frequency generator in combination with a quartz-crystal band-pass filter which sets the bandwidth  $\Delta f$  of the noise. The filter operates at a frequency of a few MHz and the noise signal is subsequently mixed with a fixed-frequency signal close to the hyperfine transition at 6.8 GHz to match the output coupling frequency.

After propagating a distance of 36 mm the atoms enter the ultra-high-finesse optical cavity (see Fig. 1). The cavity consists of two identical mirrors separated by  $178 \mu\text{m}$ . Their radius of curvature is  $77.5 \text{ mm}$ , resulting in a Gaussian  $\text{TEM}_{00}$  mode with a waist of  $w_0 = 26 \mu\text{m}$ . The coupling strength between a single Rb atom and the cavity field is  $g_0 = 2\pi \times 10.4 \text{ MHz}$  on the  $F = 2 \rightarrow F' = 3$  transition of the  $\text{D}_2$  line. The cavity has a finesse of  $3 \times 10^5$  and the decay rate of the cavity field is  $\kappa = 2\pi \times 1.4 \text{ MHz}$ . The spontaneous decay rate of the atomic dipole moment is  $\gamma = 2\pi \times 3 \text{ MHz}$ . Since  $g_0 \gg \kappa, \gamma$  we operate in the strong coupling regime of cavity quantum electrodynamics (QED). The cavity resonance frequency is stabilized by means of a far-detuned laser with a wavelength of  $830 \text{ nm}$  using a Pound–Drever–Hall locking scheme.

The cavity is probed by a weak, near-resonant laser beam whose transmission is monitored by a single photon counting module. We find a shot-noise-limited transmission of photons through the empty cavity. The presence of an atom inside the cavity results in a drop of the transmission. The intensity and the frequency of the detection laser are optimized to yield a maximum detection efficiency for the released atoms

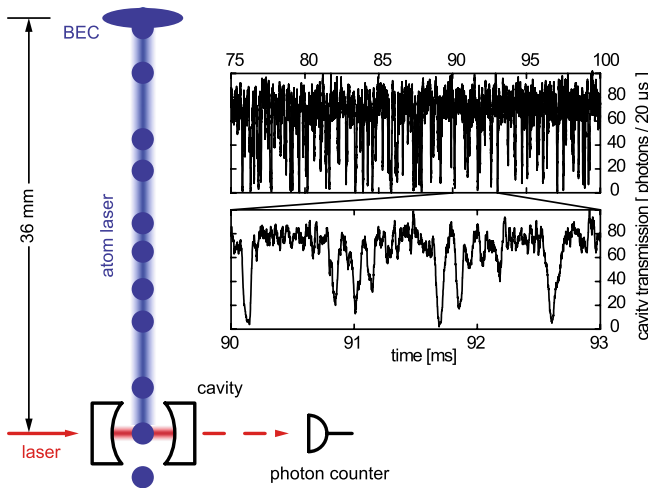


**FIGURE 1** Schematic view of the experimental setup. A Bose–Einstein condensate (BEC) is produced 36 mm above an ultra-high-finesse optical cavity. Using microwave output coupling we extract an atomic beam from the condensate, which passes through the cavity. The intensity of a laser beam probing the cavity is modified by the presence of a single atom inside the cavity, resulting in the characteristic dips of the cavity transmission

that is  $(23 \pm 5\%)$  [14]. This number is primarily limited by the size of the atom laser beam, which exceeds the cavity mode cross section. The atoms enter the cavity with a velocity of  $84 \text{ cm/s}$ . The resulting dead time of our detector of approximately  $70 \mu\text{s}$  is short compared to the time scale of the correlations, which allows us to perform Hanbury Brown and Twiss type measurements with a single detector [18].

We record the cavity transmission for the period of atom laser operation (typically  $0.5 \text{ s}$ ) and average the photon counting data over  $20 \mu\text{s}$ . Using a peak detection routine we determine the arrival time of atoms in the cavity, requiring that the cavity transmission drops below the empty cavity value by at least four times the photon shot noise.

### 3 Results

We first investigate the distribution function of the time intervals between successive atom counting events. This represents a ‘start–stop’ measurement, where a time counter is triggered by an atom detection event and stopped by the next detection event [3]. From the histogram of the measured time intervals, we obtain the conditional probability  $p(t|t + \tau)$  of detecting the next atom a time  $\tau$  later than an initial atom observed at  $t$ . These exclusive pair correlations, for which we restrict ourselves to consecutive atom detection events, are distinguished from the non-exclusive pair correlations measured by the second-order correlation function  $g^{(2)}(\tau)$ . There, the pairwise time differences between all atoms are evaluated.

For an average count rate  $\nu$  the conditional detection probability density for a coherent beam is given by [19]

$$p_{\text{coh}}(0|\tau) = \nu \exp(-\nu\tau). \quad (2)$$

In contrast, for a thermal state of bosons one finds [19]

$$p_{\text{th}}(0|\tau) = \frac{2\nu}{(1 + \nu\tau)^3}. \quad (3)$$

For  $\tau = 0$  the thermal probability density is twice as large as the coherent probability density. This reflects the increased thermal fluctuations and the bunching behavior in pair correlations of bosonic particles.

In Fig. 2 we compare our data with this theory. For the pseudo-thermal atomic beam we have chosen a bandwidth of  $\Delta f = 90 \text{ Hz}$  and analyzed time intervals short compared to the coherence time  $\tau_c = 1/\Delta f = 11 \text{ ms}$ . We normalize the measured probability by the measured count rate  $\nu_{\text{exp}} = 1.3 \times 10^3 \text{ s}^{-1}$  and fit the result with the functions given in (2) and (3), allowing for some overall scaling factor. From the fits we obtain the average count rates  $\nu = 1.4 \times 10^3 \text{ s}^{-1}$  and  $\nu = 1.6 \times 10^3 \text{ s}^{-1}$  for the atom laser beam and the pseudo-thermal beam, respectively, which compares well with the experimentally determined flux  $\nu_{\text{exp}}$  for both cases. For  $\tau = 0$  we find that the data for the atom laser beam exceed  $p(0|\tau)/\nu_{\text{exp}} = 1$  by approximately 15%. Similarly, the results for the pseudo-thermal beam exceed  $p(0|\tau)/\nu_{\text{exp}} = 2$  by approximately 30%. This could be attributed to the dead time of our detector – which is about  $70 \mu\text{s}$  [6] – during which we cannot detect a possible consecutive event. We estimate the probability for a second atom arriving within the dead time of the detector to be 5% for the atom laser beam and 10% for atoms in

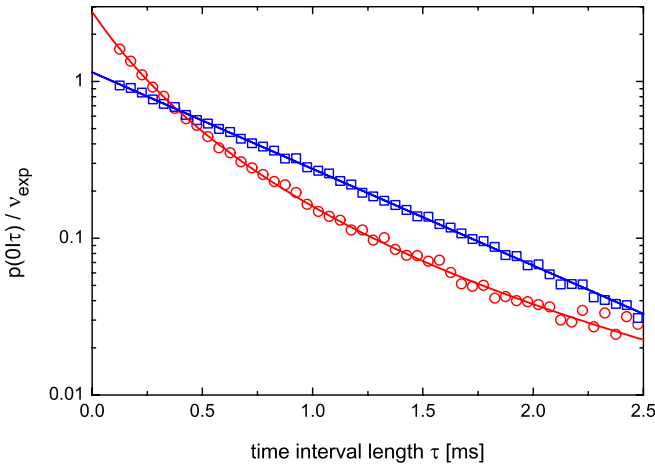


**FIGURE 2** Conditional detection probability  $p(0|\tau)$ . The frequency distribution of the time intervals between two successive atom counts is shown for the atom laser (*squares*) and for a pseudo-thermal beam with a bandwidth of  $\Delta f = 90$  Hz (*circles*). The *lines* are fits according to (2) and (3)

the pseudo-thermal beam. With this probability a later atom might falsely be identified as being consecutive to the initial event, which overestimates the number of time intervals larger than the detector dead time. Moreover, the experimental count rate is underestimated by the same factor, also contributing to the enhancement of the data above the theoretical expectation.

Next, we study the unconditional probability of a single atom detection event. The unconditional probability assumes that the timer is started at a randomly chosen time and records the time to the next atom detection event. For a coherent beam of atoms the unconditional probability for a detection event  $p(t)$  is equal to the conditional probability investigated above [19]:

$$p_{\text{coh}}(\tau) = \nu \exp(-\nu\tau). \quad (4)$$

This reflects the absence of any density correlations in a coherent atomic beam. For a thermal state one finds

$$p_{\text{th}}(\tau) = \frac{\nu}{(1 + \nu\tau)^2}, \quad (5)$$

which for  $\tau = 0$  differs from the corresponding conditional probability by a factor of 2. The physical reason for this difference lies in the bunching of thermal bosons, which enhances the detection probability only for two nearby events measured by the conditional probability. The unconditional probability measures a single-particle property and does not reveal a bunching effect. In Fig. 3 we show our measurements of the atom detection probability for a randomly chosen initial start point and find good agreement with the theoretical prediction. Similarly to the results for the conditional probability, we observe that the experimental data for  $\tau = 0$  are larger than the theoretically expected result of  $p(\tau)/\nu_{\text{exp}} = 1$  by the same relative amount as in Fig. 2. We attribute this again to the dead time of our detector, as discussed above. The apparently better data quality of Fig. 3 as compared to Fig. 2 is due to the larger number of available time intervals for the unconditional probability.

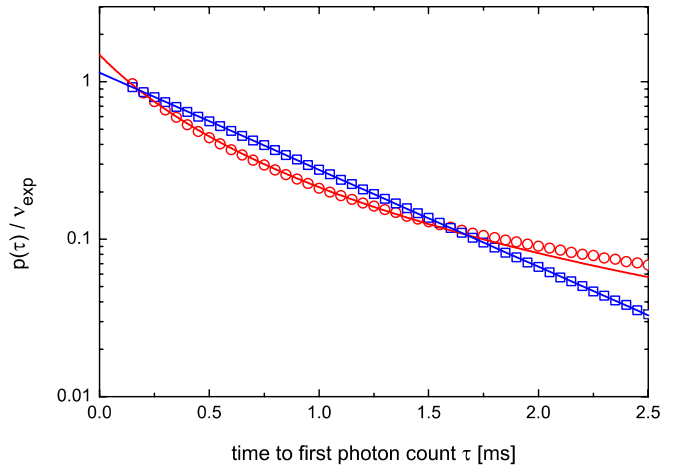


**FIGURE 3** Unconditional detection probability  $p(\tau)$ . The frequency distribution of the length of the intervals between a randomly chosen start point and the subsequent atom detection event is shown for the atom laser (*squares*) and for a pseudo-thermal beam with a bandwidth of  $\Delta f = 90$  Hz (*circles*). The *lines* are fits according to (4) and (5)

## 4 Conclusion

We have studied the time interval distribution of atom detection in an atom laser beam and a pseudo-thermal atomic beam. We have investigated both the conditional and the unconditional detection probabilities and found good agreement with the theoretical predictions. This complements the measurement of the second-order correlation function of the atomic beams [6].

**ACKNOWLEDGEMENTS** We acknowledge stimulating discussions with F.T. Arecchi and F. Brennecke, and thank R. Glauber for suggesting this experiment. This work is supported by SNF, QSIT, and the EU project OLAQUI.

## REFERENCES

- 1 R. Hanbury Brown, R.Q. Twiss, *Nature (London)* **177**, 27 (1956)
- 2 F.T. Arecchi, *Phys. Rev. Lett.* **15**, 912 (1965)
- 3 F.T. Arecchi, E. Gatti, A. Sona, *Phys. Lett.* **20**, 27 (1966)
- 4 M. Yasuda, F. Shimizu, *Phys. Rev. Lett.* **77**, 3090 (1996)
- 5 M.H. Anderson, J.R. Ensher, M.R. Matthews, C.E. Wieman, E.A. Cornell, *Science* **269**, 198 (1995)
- 6 A. Öttl, S. Ritter, M. Köhl, T. Esslinger, *Phys. Rev. Lett.* **95**, 090404 (2005)
- 7 M. Schellekens, R. Hoppeler, A. Perrin, J.V. Gomes, D. Boiron, A. Aspect, C.I. Westbrook, *Science* **310**, 648 (2005)
- 8 E. Altman, E. Demler, M.D. Lukin, *Phys. Rev. A* **70**, 013603 (2004)
- 9 S. Fölling, F. Gerbier, A. Widera, O. Mandel, T. Gericke, I. Bloch *Nature (London)* **434**, 481 (2005)
- 10 M. Greiner, C.A. Regal, J.T. Stewart, D.S. Jin, *Phys. Rev. Lett.* **94**, 110401 (2005)
- 11 L. Cacciapuoti, D. Hellweg, M. Kottke, T. Schulte, W. Ertmer, J.J. Arlt, K. Sengstock, L. Santos, M. Lewenstein, *Phys. Rev. A* **68**, 053612 (2003)
- 12 D. Hellweg, L. Cacciapuoti, M. Kottke, T. Schulte, K. Sengstock, W. Ertmer, J.J. Arlt, *Phys. Rev. Lett.* **91**, 010406 (2003)
- 13 M. Köhl, T.W. Hänsch, T. Esslinger, *Phys. Rev. Lett.* **87**, 160404 (2001)
- 14 A. Öttl, S. Ritter, M. Köhl, T. Esslinger, *Rev. Sci. Instrum.* **77**, 063118 (2006)
- 15 T. Esslinger, I. Bloch, T.W. Hänsch, *Phys. Rev. A* **58**, R2664 (1998)
- 16 I. Bloch, T.W. Hänsch, T. Esslinger, *Phys. Rev. Lett.* **82**, 3008 (1999)
- 17 W. Martienssen, E. Spiller, *Am. J. Phys.* **32**, 919 (1964)
- 18 L. Mandel, E. Wolf, *Rev. Mod. Phys.* **37**, 231 (1965)
- 19 R.J. Glauber, in *Laser Handbook*, vol. 1, ed. by F.T. Arecchi, E.O. Schulz Dubois (North-Holland, Amsterdam, 1972), Chapt. A1, pp. 1–43